R. Albarracin, G. Robles, J.M. Martinez-Tarifa, J. Ardila-Rey (2015). Separation of sources in radiofrequency measurements of partial discharges using time-power ratios maps, in *ISA Transactions* [Available online 18 May 2015].
http://dx.doi.org/10.1016/j.isatra.2015.04.006

*

Universidad
Carlos III de Madrid

Separation of sources in radiofrequency measurements of partial discharges using time-power ratios maps

R. Albarracin[a,*], G. Robles[a,*], J.M. Martinez-Tarifa[a], J. Ardila-Rey[b]

[a] *Departament of Electrical Engineering, Universidad Carlos III de Madrid, Leganés - 28911, Spain.*
[b] *Departament of Electrical Engineering, Universidad Técnica Federico Santa María, Santiago de Chile, Chile*

*Corresponding author
Email addresses: ralbarra@ing.uc3m.es (R. Albarracin), fax: 34916249430 (R. Albarracin), grobles@ing.uc3m.es (G. Robles), 34916245922 (G. Robles), jmmtarif@ing.uc3m.es (J.M. Martinez-Tarifa), jorge.ardila@usm.cl (J. Ardila-Rey)

Separation of sources in radiofrequency measurements of partial discharges using time-power ratios maps

Abstract

Partial discharges measurement is one of the most useful tools for condition monitoring of high-voltage (HV) equipment. These phenomena can be measured on-line with antennas provided that the signal to noise ratio is improved by reducing common radiofrequency (RF) emission. One approach to this problem is the use of specific sensors like Vivaldi antennas which reject FM radio and low-frequency TV broadcasting bands. Additionally, the application of advanced signal processing techniques is paramount to separate noise and interferences from the signals of interest. In this paper, the power ratios (PR), a technique based on the power distribution of the incoming signals in frequency bands, is used to characterize different sources of PD and electromagnetic noise (EMN). The calculation of the time length of the pulses is introduced to separate signals where the PR alone do not give a conclusive solution. Thus, if several EM sources could be isolated and previously calibrated, it is possible to detect pulses that correspond to other events, quite possibly from PD activity.

Keywords: Partial discharges, dielectric materials, condition monitoring, RF measurements, VHF and UHF measurements, Vivaldi antennas, spectral power.

1. Introduction

The insulation systems of electrical assets are subjected to mechanical, thermal and electrical stresses that degrade their behaviour and can lead to unexpected equipment outages and failures, such as in rotating machines, Sharifi and Ebrahimi (2011). Knowing the condition of the insulation is key for the reliability of power systems, Gill (2008). Partial discharges (PD) are low-energy ionizations in sites where highly divergent fields are present, Boggs (1990) so they represent a measurable manifestation of electrical stress and

a symptom of other problems in the electrical asset. They are classified into three groups: corona, surface and internal, Kreuger (1989). Corona PD, often occur in sharp metallic structures under high-voltage stress. Surface PD may also occur in inhomogeneous locations on dielectrics when there exist a tangential component of the electric field parallel to the dielectric surface. And, finally, the most harmful PD for electrical insulation are internal, occurring in gas filled cavities inside the dielectric, due to imperfections in the manufacturing process, installation or external damages. In addition, its continued activity gradually degrades the insulation system in which they occur leading to a total discharge and the breakdown of the electrical equipment. Therefore, the detection of PD activity is an important test for determining the quality of the insulation system, IEC-60270 (2000). Moreover, the analysis of partial discharges helps to perform a correct condition-based maintenance (CBM) of power system assets such as air-insulated (AIS) and gas-insulated substations (GIS), transformers, power cables, motors and generators.

One immediate consequence of the PD activity is an electromagnetic (EM) emission in the very-high-frequency (VHF) and ultra-high-frequency (UHF) bands, 30—300 MHz and 300—3000 MHz, respectively, that can be measurable in RF with disc couplers and antennas, Judd et al. (1995); Shibuya et al. (2010). The use of EM sensors can be applied to any type of insulating material with the advantage of not needing a galvanic connection to the equipment when compared with capacitive and inductive sensors. Moreover, the nature of an insulating dielectric can be related to the frequency band emitted by the PD, being their energy higher at high frequencies for stronger dielectrics than for weaker insulations, Moore et al. (2005).

On the other hand, the advantage of galvanic insulation turns into a disadvantage when the phase of the sinusoidal voltage is needed to find out what type of PD is active. This is usually done with phase resolved partial discharge (PRPD) patterns where the amplitude of the pulse versus the phase referred to the applied voltage are plotted, and the type of PD is identified through the pattern it draws, Kreuger (1989). Additionally, there is not a clear relationship between the power emitted by the PD and the power received by the antenna. This loss of information makes it difficult to separate the signals of interest from other interferences (considered, henceforth, as noise). The electromagnetic noise (EMN) can be classified into several categories:

• Continuous sinusoidal noise from communication systems such as: FM radio, digital TV, Digital Audio Broadcasting (DAB), Global System for

Mobile communications (GSM) and Wi-Fi, which can hide the sources of PD and even can be superimposed to PD pulses. All sources together emit energy in a broadband so their filtering can be laborious as well as the subsequent separation from PD.

• Stochastic noise, random both in time and amplitude such as: corona in air, that can emit energy up to 500 MHz, though in most cases they only reach 250 MHz, Tenbohlen et al. (2008), sparking and lamp ignition;

• Periodic-pulsing noise from thyristor operation, i.e. inverters in electrical motors and voltage or current regulated sources.

For these reasons, the characterization of PD in RF is an open and current research topic whose challenge is the possibility of separating di erent EM sources. All current methods are based on the frequency characteristics of the emitted signals and what changes is the way they represent the diferences. In some cases, these representations are based on triangles in which every side is a frequency band at low, medium and high frequencies. In Baker et al.(2013), the curves represented in these ternary plots are not absolute values for the magnitude of every source but relative values to each of the sources. In Gao et al. (2013), the representation is again in a ternary plot, this time with the energy of the signals. In Peiqing et al. (2012), the representation is based on a time-frequency map already used in measurements with high-frequency transformers in conventional methods with PRPD. Finally, in Umamaheswari and Sarathi (2011), support vector machines are used to classify signals but a previous training of the SVM is needed.

The proposed algorithm represents the diferences in frequency in only two dimensions so one of its main characteristics is its simplicity and the facility to extract conclusions from the representation map. Moreover, when the spectra are very similar and cannot separate the sources, it is complemented with the time duration of the signals. In this sense, the aim is that the separation technique integrates calculations with low computational load to open the possibility to be implemented in Field-Programmable Gate Arrays (FPGA) or in low-cost microprocessors.

In this paper, the use of a specific sensor together with an ad-hoc signal-processing technique are proposed to separate several PD sources and electromagnetic noise (EMN). First, Vivaldi antennas, due to their constructive nature, allows to mitigate FM radio and low-frequency TV broadcasting bands. Second, the spectral Power Ratios (PR), Ardila-Rey et al. (2013) were selected as a low computational load tool to isolate the measured sources. With this aim, measurements of corona and surface PD have been carried

out when two EM sources of disturbances are present. Their power spectral content in two bands of frequency (low-frequency and high-frequency) is plotted in a two-dimension map to separate the signals. It may occur that some EM sources have power in the same frequency bands so they cannot be easily separated. The observation of the signals shows that certain powerful interferences such as sparking due to relays and lamps ignition always have long duration pulses while their frequency content remains in the same band as PD. Hence, this paper proposes the use of the time duration of the pulses as a third variable when two dimensions are not successful in the separation of the sources. Moreover, if several EM sources are previously characterised, it is possible to identify pulses from other sources that very likely could come from PD activity.

2. Vivaldi antenna

Vivaldi antennas are aperture-planar antennas that use two pieces of copper, each one aside of a dielectric substrate, Gibson (1979). This sensor is a waveguide, or slot line, of small size integrated into a dielectric substrate and an appropriate transition from a feeding transmission line installed in the antenna as depicted in Figure 1. These antennas are not resonant in nature and broad bandwidth can be achieved with low return losses by optimizing the profile of the slot and the feeding network. Moreover, this antenna has a directive pattern with linear polarization that allows to be more selective in pulse acquisitions if the sensor is set pointing to the EM emitter.

In this case, a Vivaldi antenna with a total size of 9 cm $\times$ 12 cm was originally designed and optimized to operate centred around 2 GHz. The dimensions of this sensor are chosen according to the restrictions summarized in Janaswamy and Schaubert (1985) and to operate in compliance with the requirements of the measurement of PD in UHF. The antenna was manufactured by photolithography in a FR4 dielectric substrate with a thickness of 1.5 mm. Not only is this sensor an inexpensive alternative to log-periodic antennas, but also its behaviour is better than log-periodic and monopole antennas, Robles et al. (2013). The reason is that this Vivaldi antenna, adapted for high frequencies, can also measure EM pulses with low-frequency content where corona and surface PD emits power. Thus, these type of antennas mitigate the background interference of FM radio and the low frequencies band of TV broadcasting and, furthermore, they are able to measure PD

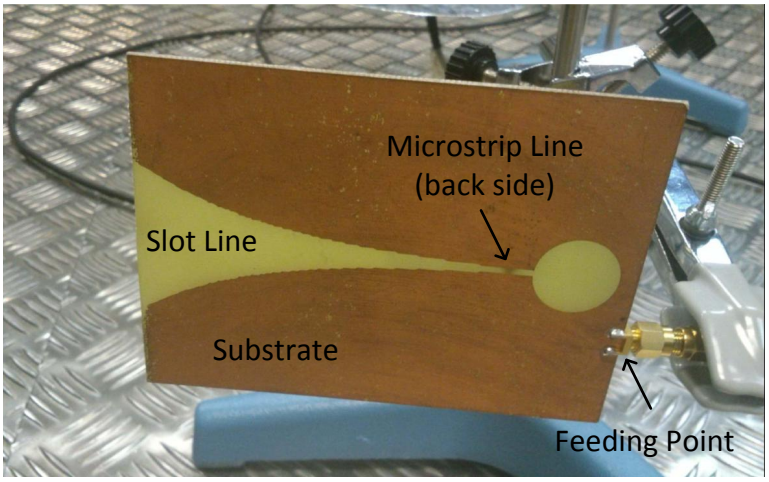

Figure 1: Vivaldi antenna layout.

in a broader band of frequencies than monopole antennas because of their non-resonant nature.

The emitter-channel-receiver system in which the antenna works can be represented by a quadrupole by using the scattering parameters, Balanis (2005). In this equivalent circuit, the return losses of the antenna are obtained from the measurement of the reflection parameter, S_{11}. When S_{11}=0 dB all the power is reflected and for values more negatives than -10 dB the sensor is considered to be matched. To measure the return losses for the manufactured prototype, an Agilent Technologies E8364B Network Analyser is used and its reflection parameter is shown in Figure 2. As it can be seen, the antenna is matched in the range between 1.3 GHz and 3 GHz. Besides, the antenna has S_{11} values close to -10 dB in the 0.7—1.2 GHz range and between -5 dB and -8 dB in the 0.6—0.7 GHz range which permits to acquire pulses with power at those frequencies, however mitigated. For frequencies lower than 0.4 GHz, the reflection parameter is greater than -2 dB, so the Vivaldi antenna works as a high-pass filter. Thus, frequency components from FM radio (the EM noise source with higher amplitude) are attenuated in more than 15 dB compared to other high-frequency components.

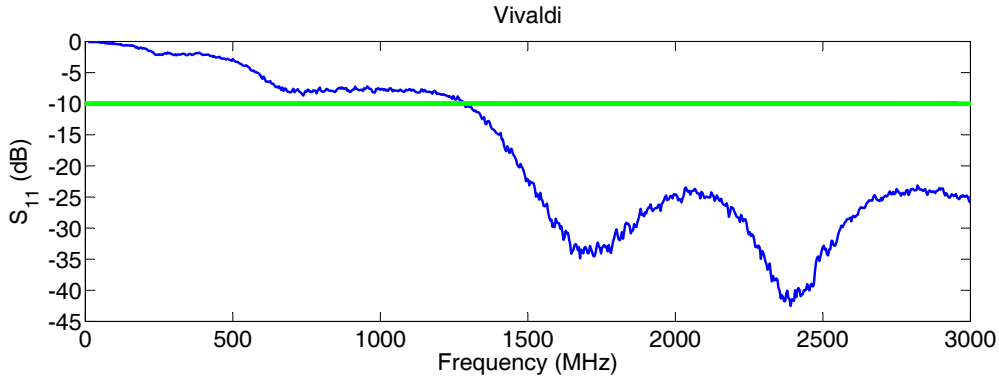

Figure 2: Reflection parameter S_{11} of the Vivaldi antenna.

3. Experimental setup

Partial discharges were created with two test objects specifically designed to generate surface and corona pulses when high-voltage is applied. The HV source is a Schleich BV 702210 transformer with a GLP1-e HV control module that can reach up to 18 kV, greater than the partial discharge inception voltage (PDIV) of the test objects. Every test object was previously tested in a setup according to the indirect circuit in Standard IEC-60270 and PD were acquired with a commercial PD analyser to register and verify the PD activity. During the measurements, two RF external perturbations were activated to study their influence in simultaneous acquisitions from the two PD sources. A laptop Wi-Fi receptor was switched on and a set of six lamps with three fluorescent lamps of 18 W each one were turned on and off during the measurements. The antenna was placed at a distance of 1 m from the test objects and connected to a Tektronix DPO 7254 oscilloscope with a sampling frequency of 40 GS/s and a bandwidth of 2.5 GHz. Each of the elements described above are shown in Figure 3.

4. Test objects design

The first test object is an electrode connected to the HV source placed on a layer of polyethylene. This configuration simulates the type of defect that can occur on the interface of two dielectrics, usually between solid dielectric and air. It is very common to find these surface PD on contaminated surfaces of dielectrics and between windings of electrical machines such as motors and

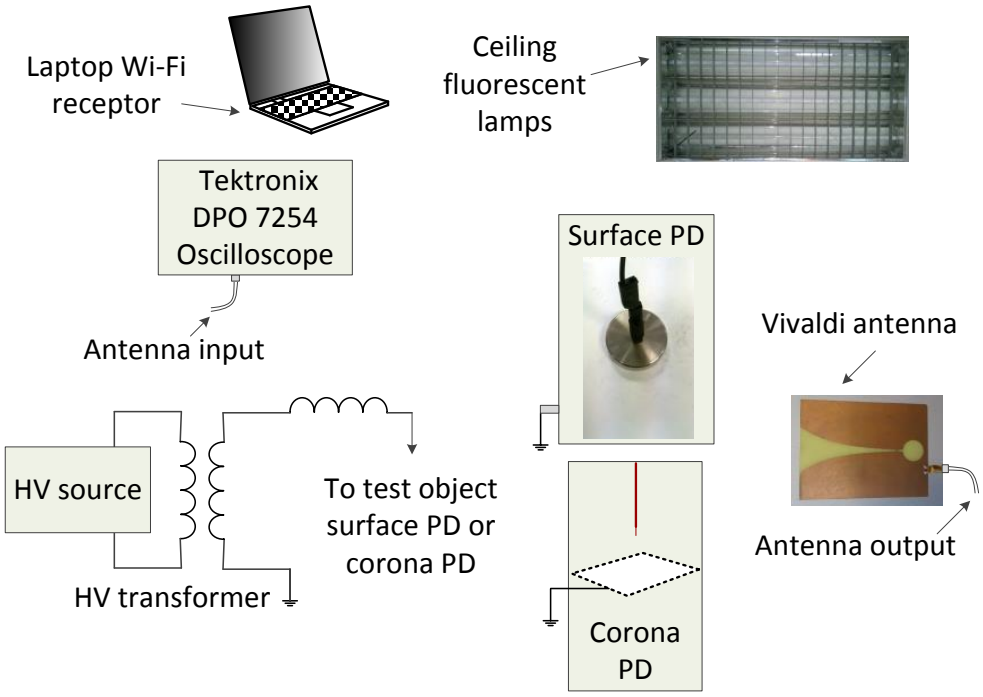

Figure 3: Experimental setup for measuring corona, surface PD and two kinds of EMN sources using a Vivaldi antenna.

other metals under electric stress. In this case, the PDIV was found to be above 1.4 kV, so the applied voltage was 1.5 kV.

The second test object consists of a copper wire 0.2 cm in diameter sharp-ended and separated 2 cm from ground. This test object represents corona PD that may appear on sharp elements when HV is applied in electrical equipment. The PDIV was found to be above 12 kV for positive corona and the applied voltage was 13 kV where there were a high activity of corona PD that could be measured by the antenna.

In both cases, the activity and the type of discharge was checked with the commercial PD acquisition system confirming surface PD in the first case and corona PD for the second, as can be seen in their phase-resolved partial discharge patterns in Figure 4, Kreuger et al. (1993).

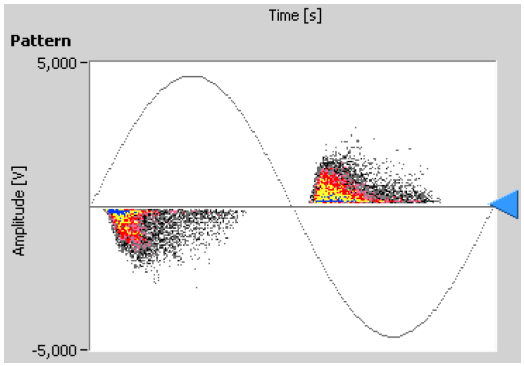

(a) Polyethylene sheet at 1.5 kV.

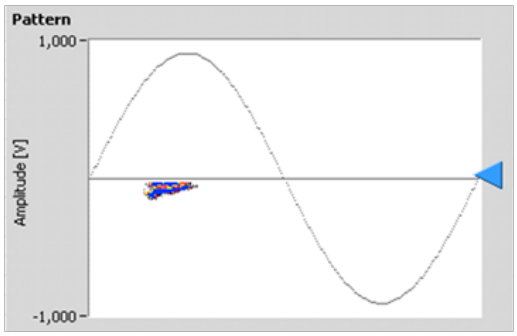

(b) Point-plane at 13 kV.

Figure 4: PRPD pattern of a) Surface PD on Polyethylene sheet and b) Corona PD in point-plane configuration.

5. Signal processing

The aim of the algorithm is to extract frequency characteristics that can help to distinguish between signals by using the PR maps and to complement this technique with the time duration of the pulse when the frequency characteristics are not sufficient to separate events.

The previous step is to normalize the signal with time, $s(t)$, using:

$$\tilde{s}(t) = \frac{s(t)}{\sqrt{\int_0^T s(t)^2 dt}} \tag{1}$$

with T the time window in which the event is registered and $\tilde{s}(t)$ is the normalised signal.

5.1. Spectral power analysis

The PR technique uses two bands of frequency where there are significant differences between signals, Ardila-Rey et al. (2013). In this case, the accumulated spectral power is:

$$\%PRL = \sum_{f=f1_L}^{f2_L} \left|\tilde{S}(f)\right|^2 \times 100 \tag{2}$$

$$\%PRH = \sum_{f=f1_H}^{f2_H} \left|\tilde{S}(f)\right|^2 \times 100 \tag{3}$$

considering that the total power of the signal is 1 because it has been normalized. PRL and PRH are the power ratios for the low-frequency, $[f1_L, f2_L]$, and high-frequency, $[f1_H, f2_H]$, bands, respectively. The two bands, can be set according to the frequency characteristics of the signal. $\left|\tilde{S}(f)\right|$ is the fast Fourier transform (FFT) value of the PD normalized pulse.

The PRL and PRH parameters are plotted in a 2D map to separate EM sources different from noise and EMN. Once the separation is satisfactory, the signals in a cluster are selected and represented in a PRPD pattern, Ardila-Rey et al. (2013). Unfortunately, in most cases, when PD measurements are done in RF, it is not possible to have access to a grid voltage reference to obtain the PRPD. To overcome this drawback, the approach in this paper is based on the previous characterization of all EM sources through a PR map when all PD sources are inactive. Then, other EM sources that may appear later placing the antenna close to a potential PD source, will very likely come from the activity of PD and will have their position in the map.

5.2. Signal time duration

In some cases, two or more EM sources can be overlapped and it may be necessary to obtain additional information from the time characteristics of the measured pulse such as its total time duration. Once calculated, it may be included in the PRL-PRH map to add a third dimension to enable a better separation between clusters.

The effective pulse width (t_{eff}), is used to calculate the equivalent time length from each pulse. This time corresponds to the width of a rectangular pulse with the same peak as the squared signal and whose integral gives the

same energy, so both have the same area. The time t_{eff} is calculated as follows:

$$t_{eff} = \frac{\int_0^T \tilde{s}(t)^2 dt}{\tilde{s}(t)^2_{max}} = \frac{1}{\tilde{s}(t)^2_{max}} \tag{4}$$

where the numerator of the fraction is the integral value of the pulse for the entire acquisition window, being 1 because it is normalized and $\tilde{s}(t)_{max}$ is the maximum value of the signal.

6. Measurements and results

Partial discharges from each test object, Wi-Fi interferences and lighting of fluorescent lamps were acquired simultaneously with the Vivaldi antenna. The EMN is also included from other acquisitions campaign. The measuring method is performed so as to obtain reliable and comparable acquisitions. The oscilloscope registered and saved 1000 signals in the time domain with a sampling frequency of 5 GS/s and a time window of $T = 0.5$ μs.

6.1. Background noise and disturbances characterization

Before the acquisition of PD, the background EMN has to be characterized and identified. Its averaged spectrum, represented in Figure 5, is obtained from their normalized pulses and the frequency bands of interest are defined in Figure 6 up to 2.5 GHz. As it can be seen from its spectrum, Figure 5, these pulses have a poor response at low frequencies as expected, so the FM radio effect is notably reduced. This is a clear advantage both in time and frequency when acquiring PD in RF with the Vivaldi antenna.

Other EM sources of disturbance can difficult the measurement of PD such as sparking and relay commutations. Pulses from the lighting of fluorescent lamps are acquired when the switch is turned on. When the electronic ballast that feeds the lamp is started, produces fast arcs and sparks that are measurable in RF. Note that, fluorescent lamps during its normal operation and when they are switched off do not emit measurable pulses in RF. An energy normalized pulse and its spectrum are presented in Figures 7a and 8a, respectively.

The second EM source of disturbance studied is a Wi-Fi receiver in a laptop, that is activated when the measurement campaign is started and is close enough to the antenna in the laboratory so their pulses have sufficient amplitude to trigger the oscilloscope acquisition. This kind of EMN source

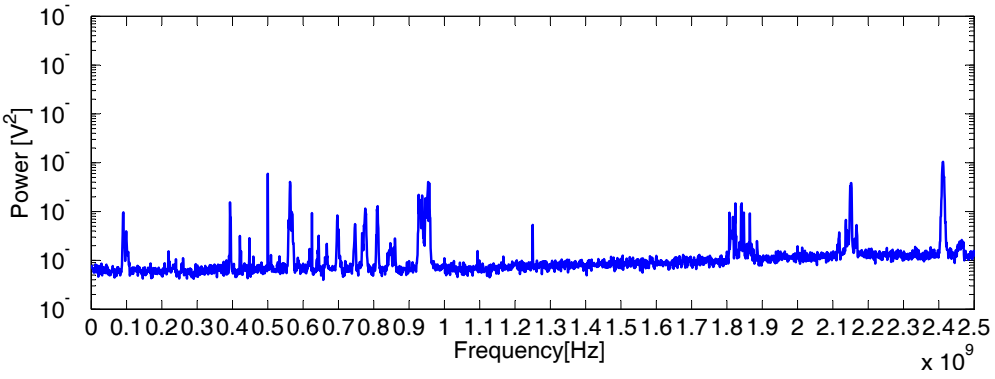

Figure 5: Background EMN measured by Vivaldi antenna.

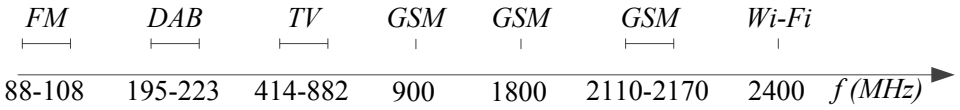

Figure 6: Frequency bands of the background EMN.

can be present in field measurements when a laptop is necessary for the RF acquisition system. Its energy normalized pulse and its spectrum are shown in Figures 7b and 8b, respectively.

Due to the fact that both disturbances, Wi-Fi (when the receiver is activated) and fluorescent lamp emissions, can be controlled they can be studied separately and simultaneously to corroborate where their clusters are located in the 2D and 3D PR maps.

Since the frequency ranges in which the separation on the PR map is satisfactory are not known, it is necessary to calculate the FFT of all pulses and compare the most representative spectra with the EMN floor and to each other. This will determine which frequency bands have significant changes. For all cases studied, a good separation is achieved with the following frequency values: f_{1L}=120 MHz, $f_{2L} = f_{1H}$=850 MHz and f_{2H}=1700 MHz.

All disturbances are plotted together in a PR map and in a PR-time map, Figures 9a and 9b, respectively. As it can be seen, it is possible to identify three different clusters: background EMN, Wi-Fi receiver and fluorescent lamp emissions.

The background EMN is the easiest to locate because it is always present

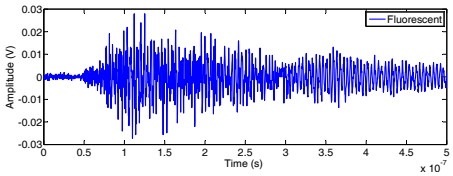

(a) Fluorescent lamp ignition pulse.

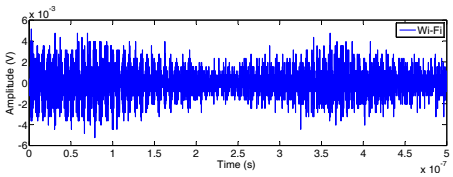

(b) Wi-Fi pulse.

Figure 7: RF pulses measured by the Vivaldi antenna: fluorescent lamp ignition and Wi-Fi.

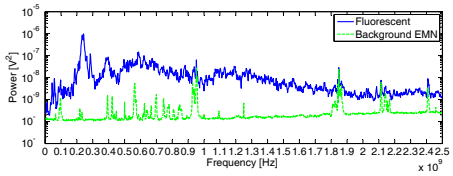

(a) Fluorescent lamp ignition spectrum.

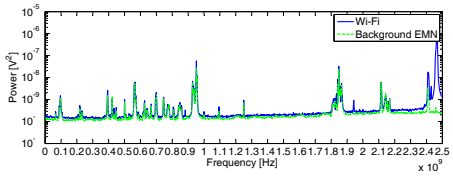

(b) Wi-Fi spectrum.

Figure 8: Power spectrum of RF pulses measured by the Vivaldi antenna: fluorescent lamp ignition and Wi-Fi compared to the EMN floor.

and a simple measurement in an open area without other emission will be enough to characterize its position. For the low and high frequency intervals given above, the EMN cluster has the following parameters PRL=10—31 %, PRH=18.7—62.8 % and t_{eff}=18—49 ns, with an average value of 32.6 ns. Notice, that being interferences from radio and TV broadcasting, the

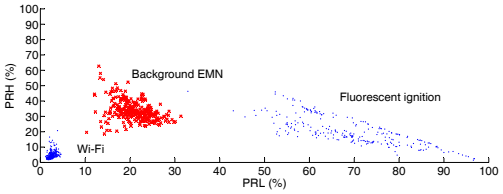

(a) 2D map for background EMN, Wi-Fi and fluorescent lamp ignition.

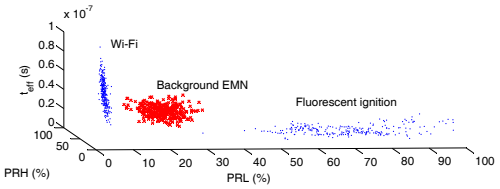

(b) 3D map for background EMN, Wi-Fi and fluorescent lamp ignition.

Figure 9: a) PR and b) PR-time maps for the background EMN, Wi-Fi and fluorescent lamps emissions measured by the Vivaldi antenna.

equivalent time durations will be long.

Wi-Fi is a 2.4 GHz modulated signal so its power is almost not taken into account for the chosen intervals. Then, it is shown as a cluster located at low PRL and PRH values, from 1.5—6 % while the equivalent time duration is the longest, with an average value of 58 ns.

The fluorescent lamps ignition pulses, and in general, sparking and relay commutation, are characterized by short to medium duration pulses and high dispersion of power in all the band of frequencies. In this case t_{eff}=3.6—33 ns, and 14.8 ns of average value, with high PRL values in the range of 40—98%.

6.2. Measurements with the antenna and separation of multiple EM sources

Once the background EMN and the disturbances have been characterized, partial discharges are measured simultaneously with disturbances by applying HV to the corona and the surface PD test objects individually. During the acquisitions, the fluorescent lamps are successively switched on and off and the Wi-Fi receptor is activated.

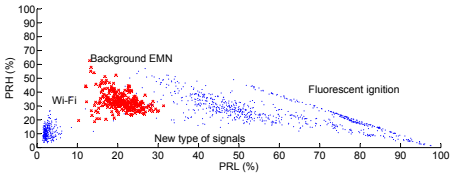

(a) PR map.

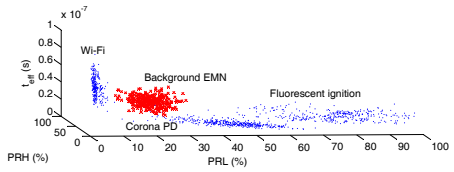

(b) PR-time map.

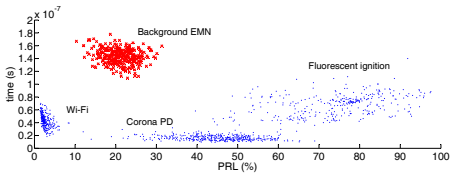

(c) PRL-time map.

Figure 10: a) Power ratio map, b) PR-time map and c) PRL-time map for fluorescent lamp ignition pulses, Wi-Fi, corona PD source and EMN.

6.3. Pulse separation

6.3.1. Corona PD, Wi-Fi and fluorescent lamps ignition

In this experiment all disturbing sources are active with the point-plane test object energized at 13 kV. The position of all disturbances does not change so it is clear that the new cluster that appears in the plot in Figure 10a comes from the new corona EM source.

This corona cluster intersects slightly with the fluorescent lamp and EMN clusters and the border is not clear in some areas. Even under these circumstances, the PR map representation would be enough to separate all sources. If the pulse duration is added as a third dimension, Figure 10b, the clusters appear clearly separated and it is possible to distinguish the multiple sources. Moreover, the PRL-time view of the 3D map, Figure 10c, gives a better perspective of all events in which the clusters are even more separated.

Corona PD are characterized by short time durations with t_{eff}=2.8—18

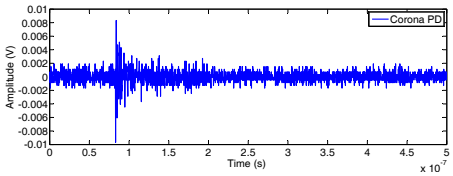

(a) Corona PD pulse.

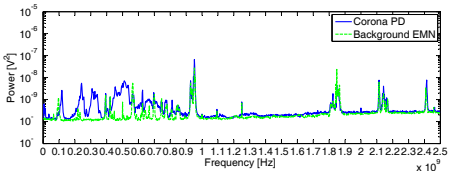

(b) Corona PD spectrum.

Figure 11: RF pulse from the first PD source and its spectrum.

ns, while its average value is 7.3 ns, so they are clearly distinguishable from other clusters. The power is also dispersed through all the spectrum from 100—900 MHz, approximately so the pulses are represented in a cluster in the ranges of PRL=22—70 %, PRH=14.6—57 %. One example of a corona pulse in the time and frequency domains are represented in Figure 11a and 11b, respectively.

6.3.2. Surface PD, Wi-Fi and fluorescent lamp ignition

This experiment includes the effect of the surface partial discharges in the polyethylene test object. Notice that the PRL-PRH map in Figure 12a shows that the interferences (Wi-Fi receptor, the fluorescent lamp ignition and the background EMN emissions) are located in the same zones as before because the frequency intervals, PRL (120—850 MHz) and PRH (850—1700 MHz), have not been changed. Unfortunately, the cluster of surface discharges is located in an area that it is already occupied by two other sources, especially the background EMN, so the final cloud of points is impossible to separate. Including the time duration t_{eff}, Figures 12b and 12c, the clusters appear separated and surface PD with very short time durations t_{eff}=0.7—5.7 ns, being 2 ns its average value, are located at the bottom of the 3D map. These effective times are the shortest of all measured events, so even having power in coincident bands with other sources (PRL=6—25 % and PRH=9—41 %) surface discharges can been separated.

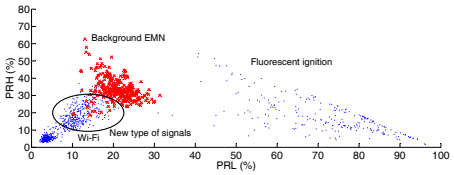

(a) PR map.

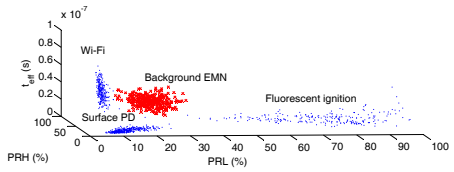

(b) PR-time map.

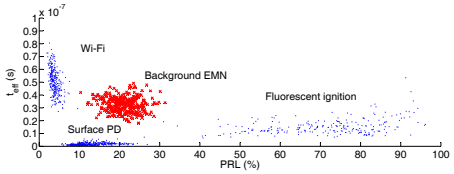

(c) PRL-time map.

Figure 12: a) Power ratio map, b) PR-time map and c) PRL-time map for fluorescent lamp ignition pulses, Wi-Fi, surface PD source and EMN.

Figure 13a shows a surface PD pulse where its short duration can be appreciated. Finally, Figure 13b shows that it has power in all the frequency band.

To summarize, all results are included in Table 1, where the values of PRL, PRH and average time duration for each EM source are included.

Table 1: Summary of time-power ratios for the EM sources measured.

Source	PRL (%)	PRH (%)	t_{eff} average (ns)
Background EMN	10—31	18.7—62.8	32.6
Wi-Fi	1.5—6	2—20	58
Fluorescent ignition	40—98	2—50	14.8
Corona PD	22—70	14.6—57	7.3
Surface PD	6—25	9—41	2

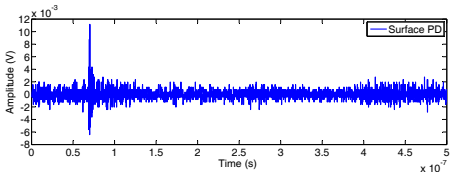

(a) Surface PD pulse.

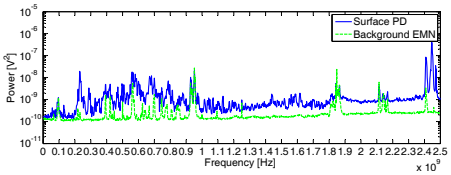

(b) Surface PD spectrum.

Figure 13: RF pulse from the second PD source and its spectrum.

7. Conclusions

The main drawback of the EM PD condition monitoring is that, in most cases, it is not possible to obtain a PRPD because there is not voltage grid synchronisation. In this paper, it has been found that all sources have characteristics that permit their recognition and differentiation from each other. The Wi-Fi has the larger time duration followed by the EMN and the fluorescent lamp ignition emissions. The fluorescent lamp pulse has the highest amplitude, reaching 30 mV, whereas the EMN has the lowest, lower than Wi-Fi pulses at 6 mV. Generally, PD pulses are characterized by extremely short rise times that are translated into electromagnetic pulses with very short time lengths. Corona and surface PD signals have mid-range amplitudes and the shortest durations. Only in the case of having important multipath propagations, these pulses would be longer in time and the antenna should be moved around for an optimum characterization. Considering all these characteristics, the separation is more effective if the differences in time are taken in account.

The power distribution in frequency for the pulses from the fluorescent lamp is located in a wide band mainly from 300 MHz to 2500 MHz. On the other side, the Wi-Fi pulses have power mainly for 2.4 GHz. Corona PD emit power in the 100—900 MHz band though most of it is in the 200—600 MHz range. Surface PD power in the polyethylene test object ranges from

200 MHz to 2500 MHz.

From these results, it is clear that it is possible to separate clusters and if the EM disturbances are known and catalogued, PD can also be identified. Besides, PD from two controlled PD test objects can also be separated and further processed to identify their nature.

In summary, if several of the EM disturbance sources are isolated and previously characterised, it is possible to detect pulses that correspond to other events, quite possibly from PD activity. In the separation process, it is possible that several clusters are overlapped in the PR maps but including the pulse duration, the clouds appear separated in the time axis. Then, the pulses from the non-characterised clusters can be analysed in time and frequency to identify them.

Acknowledgements

Tests were done in the High-Voltage Research and Test Laboratory (LINEALT) at Universidad Carlos III de Madrid.

8. References

J. Ardila-Rey, J. Martinez-Tarifa, G. Robles, and M. Rojas-Moreno. Partial discharge and noise separation by means of spectral-power clustering techniques. *Dielectrics and Electrical Insulation, IEEE Transactions on*, 20(4):1436–1443, August 2013. ISSN 1070-9878. doi: 10.1109/TDEI.2013.6571466.

P.C. Baker, B. Stephen, and M.D. Judd. Compositional modeling of partial discharge pulse spectral characteristics. *Instrumentation and Measurement, IEEE Transactions on*, 62(7):1909–1916, July 2013. ISSN 0018-9456. doi: 10.1109/TIM.2013.2247711.

Constantine A. Balanis. *Antenna Theory: Analysis and Design*. Wiley-Interscience, 3rd edition, 2005. ISBN 047166782X.

S.A. Boggs. Partial discharge. III. Cavity-induced PD in solid dielectrics. *Electrical Insulation Magazine, IEEE*, 6(6):11–16, Nov 1990. ISSN 0883-7554. doi: 10.1109/57.63094.

Wensheng Gao, Dengwei Ding, Weidong Liu, and Xinhong Huang. Analysis of the intrinsic characteristics of the partial discharge induced by typical defects in GIS. *Dielectrics and Electrical Insulation, IEEE Transactions on*, 20(3):782–790, June 2013. ISSN 1070-9878. doi: 10.1109/TDEI.2013.6518948.

P. J. Gibson. The Vivaldi aerial. In *Microwave Conference, 1979. 9th European*, pages 101–105, Sept 1979. doi: 10.1109/EUMA.1979.332681.

P. Gill. *Electrical Power Equipment Maintenance and Testing, Second Edition*. Power Engineering (Willis). Taylor & Francis, 2008. ISBN 9781574446562.

IEC-60270. *High-Voltage Test Techniques - Partial Discharge Measurements*. 3a edition, 2000.

R. Janaswamy and D.H. Schaubert. Dispersion characteristics for wide slotlines on low-permittivity substrates (short paper). *Microwave Theory and Techniques, IEEE Transactions on*, 33(8):723–726, Aug 1985. ISSN 0018-9480. doi: 10.1109/TMTT.1985.1133064.

M.D. Judd, O. Farish, and B.F. Hampton. Broadband couplers for UHF detection of partial discharge in gas-insulated substations. *Science, Measurement and Technology, IEE Proceedings*, 142(3):237–243, 1995. ISSN 1350-2344. doi: 10.1049/ip-smt:19951699.

F. H. Kreuger, E. Gulski, and A Krivda. Classification of partial discharges. *Electrical Insulation, IEEE Transactions on*, 28(6):917–931, Dec 1993. ISSN 0018-9367. doi: 10.1109/14.249365.

F.H. Kreuger. *Partial discharge detection in high-voltage equipment*. Butterworths, 1989. ISBN 9780408020633.

P.J. Moore, IE. Portugues, and IA Glover. Radiometric location of partial discharge sources on energized high-voltage plant. *Power Delivery, IEEE Transactions on*, 20(3):2264–2272, July 2005. ISSN 0885-8977. doi: 10.1109/TPWRD.2004.843397.

Miao Peiqing, Li Xiuwei, Hu Yue, Sheng Gehao, and Jiang Xiuchen. Multi-source separation method for partial discharge detection in substations.

In *Power Engineering and Automation Conference (PEAM), 2012 IEEE*, pages 1–5, Sept 2012. doi: 10.1109/PEAM.2012.6612543.

G. Robles, R. Albarracín, J.L. Vázquez-Roy, E. Rajo-Iglesias, J.M. Mártinez-Tarifa, M.V. Rojas-Moreno, M. Sánchez-Fernández, and J. Ardila-Rey. On the use of Vivaldi antennas in the detection of partial discharges. In *Solid Dielectrics (ICSD), 2013 IEEE International Conference on*, pages 302–305, June 2013. doi: 10.1109/ICSD.2013.6619887.

R. Sharifi and M. Ebrahimi. Detection of stator winding faults in induction motors using three-phase current monitoring. *ISA Transactions*, 50(1):14 – 20, 2011. ISSN 0019-0578. doi: http://dx.doi.org/10.1016/j.isatra.2010.10.008.

Y. Shibuya, S. Matsumoto, M. Tanaka, H. Muto, and Y. Kaneda. Electromagnetic waves from partial discharges and their detection using patch antenna. *IEEE Transactions on Dielectrics and Electrical Insulation*, 17(3): 862 –871, June 2010. ISSN 1070-9878. doi: 10.1109/TDEI.2010.5492260.

S. Tenbohlen, D. Denissov, S.M. Hoek, and S.M. Markalous. Partial discharge measurement in the ultra high frequency (UHF) range. *Dielectrics and Electrical Insulation, IEEE Transactions on*, 15(6):1544–1552, December 2008. ISSN 1070-9878. doi: 10.1109/TDEI.2008.4712656.

R. Umamaheswari and R. Sarathi. Identification of partial discharges in gas-insulated switchgear by ultra-high-frequency technique and classification by adopting multi-class support vector machines. *Electric Power Components and Systems*, 39(14):1577–1595, 2011. doi: 10.1080/15325008.2011.596506.